ELSEVIER

Journal of Chromatography A, 943 (2001) 77–90

JOURNAL OF CHROMATOGRAPHY A

www.elsevier.com/locate/chroma

# Impact of the physical and topographical characteristics of adsorbent solid-phases upon the fluidised bed recovery of plasmid DNA from *Escherichia coli* lysates

Eric Thwaites, Simon C. Burton, Andrew Lyddiatt*

*Biochemical Recovery Group, Biosystems Laboratory of the Research Centre for Formulation Engineering, School of Engineering, University of Birmingham, Edgbaston, Birmingham B15 2TT, UK*

Received 27 July 2001; received in revised form 22 October 2001; accepted 22 October 2001

**Abstract**

A comparison is made of the performance of two types of adsorbent solid phases (commercially sourced Streamline composites and custom-assembled Zirblast pelliculates), derivatised with similar anion exchange chemistries and applied to the recovery of plasmid DNA from *Escherichia coli* extracts prepared by chemical lysis and coarse filtration. Streamline and Zirblast adsorbents were characterised by average particle diameters of 200 and 95 μm, densities of 1.16 and 3.85 $g/m^2$, and small ion capacities of 170 and 8 μmol/ml settled adsorbent, respectively. Detailed analysis of products and impurities in a full operational cycle of adsorption, washing, pre-elution, elution and regeneration processes was enabled by the harnessing of a battery of analyses for nucleic acid and organic solute content of feedstocks and bed effluents exploiting ultra-violet spectrophotometry, agarose gel electrophoresis and specific reactions with the fluorescent probe PicoGreen. In comparative tests operated under near identical conditions, Streamline and Zirblast adsorbents exhibited plasmid recoveries of 76 and 90% of bound product characterised by purity ratios (relative PicoGreen and $A_{254}$ estimates of mass) of 9 and 32, respectively. Conclusions are drawn regarding the specific impact of the physical and topographical characteristics of solid-phase geometry upon product throughput, achievable product purity, process time-scales and operational economics for the manufacture of plasmid DNA. 

*Keywords:* Adsorbents; Streamline adsorbents; Zirblast Agarose adsorbent; PicoGreen analyses; *Escherichia coli*; Stationary phases, LC; Fluidised bed; DNA

## 1. Introduction

There is a growing interest in the large-scale manufacture of plasmid DNA sourced in recombinant *Escherichia coli* grown in batch and fed-batch fermentations [1–3]. The starting point for the purification of plasmid DNA is commonly a complex lysate generated by chemical treatment and subsequent coarse filtration of harvested cells of *E. coli* grown in batch or fed-batch fermentations [4]. Such a complex feedstock recommends the adoption of selective fractionation processes exploiting chromatography operated in fixed or fluidised bed contactors [4,5]. However, the majority of commercial adsorbents currently available for such operations have been designed and assembled for the fractionation of

*Corresponding author. Tel.: +44-121-414-5278; fax: +44-121-414-5324.

*E-mail address:* a.lyddiatt@bham.ac.uk (A. Lyddiatt).

0021-9673/02/$ – see front matter 
PII: S0021-9673(01)01445-5

macromolecular proteins (2–10 nm largest diameter) rather than the macromolecular or nanoparticulate structures which characterise plasmid DNA (50–300+ nm largest diameter depending on solvent conditions [1–3,5,6]). Such adsorbents are likely to achieve product adsorption only at the outermost surface of particles, whilst impurities (linear fragments of DNA and RNA, proteins, endotoxins and other process antagonists) can freely penetrate the porous interior with serious implications for ligand utilisation, process timescales and repetitive adsorbent useage (discussed in Refs. [3,5]). This observation invites the specific customisation of solid-phase design to offer adsorption surfaces selectively appropriate for nanoparticulate products. Such an adsorbent might be completely or nearly solid in character, and be possessed of a solid dense core suited to the processing of particulate and/or viscous feedstocks in a fluidised bed contactor [3,5].

Herein we describe the comparative performance of a commercial porous, composite adsorbent (Streamline DEAE; [7]) with a near solid particle (ZrA DEA; [5]) custom-assembled as a zirconia core (~90 μm diameter) laminated with a thin skin (<5 μm) of 6% (w/v) agarose. A prerequisite of an understanding of the performance of these two contrasting particle geometries was the development and validation of published PicoGreen protocols [8,9] for the analysis of plasmid DNA (double-stranded, ds, DNA) in the presence of RNA, DNA and other lower molecular mass contaminants.

## 2. Experimental

### *2.1. Experimental feedstocks and reagent solutions*

Pure plasmid pTX 0161 (a 7.8-kilobase pairs (kb) dsDNA vector) was kindly supplied by Cobra Therapeutics (Keele, UK) together with coarse-filtered lysate feedstock produced according to the method of Varley et al. [4] from a common batch fermentation of the host recombinant *E. coli*. Concentrated stock solution of PicoGreen dsDNA quantitation reagent [10] was sourced from Molecular Probes (Eugene, OR, US). All other reagents were analytical grade unless stated otherwise, and were sourced from Sigma (Poole, UK).

Adsorbents were contacted with feedstocks in a 1-cm internal diameter glass Omnifit column from Soham Scientific (Cambridge, UK), furnished with a top mounted plunger and a sintered glass distributor, operated in fixed and fluidised bed mode. The physical and chemical characteristics of two adsorbents used in this work are detailed in Table 1. The chromatographic system was operated with (i) equilibration buffer (B1) comprising 0.7 *M* potassium acetate, 10 m*M* EDTA, 0.02% sodium azide and adjusted to pH 5.5 with acetic acid, (ii) wash buffer (B2) comprising 50 m*M* potassium acetate, 10 m*M* EDTA, 0.5 *M* NaCl and 0.02% sodium azide at pH 7.5 and (iii) elution buffer (B3) comprising 50 m*M* potassium acetate, 10 m*M* EDTA, 2.0 *M* NaCl and 0.02% sodium azide at pH 7.5. All samples were subsequently diluted with universal dilution buffer (UDB) comprising 50 m*M* Tris–HCl, 1 m*M* EDTA at pH 7.5.

The contactor, containing 15 cm settled bed height of adsorbent (12 ml settled bed volume) was initially fluidised using equilibration buffer (B1) in upward flow mode at a volumetric flow-rate of 1 ml/min (superficial linear flow velocity ~76 cm/h). The plunger, acting as the flow outlet, was positioned just above the top of the fluidised bed. A known volume of lysate challenge was applied at the same flow-rate followed by equilibrium buffer (B1) until the effluent absorbance reading at 254 nm ($A_{254}$) achieved zero baseline values. The flow was then reversed for elution, thus packing the adsorbent into a fixed bed configuration, with the plunger acting as the inlet located just above the packed bed. Firstly, 0.5 *M* NaCl was applied as a wash buffer (B2) to elute weakly bound contaminants including RNA fragments, and secondly, a 2.0 *M* NaCl (buffer B3) elution facilitated recovery of plasmid DNA. Cleaning in place was then carried out with successive washes of 10 settled bed volumes 0.1 *M* HCl, 0.2 *M* NaOH and equilibration buffer (B1) before flow was reversed for a subsequent cycle of fluidised bed adsorption and desorption. Bed effluents were collected as timed volumetric fractions for PicoGreen, electrophoretic and spectrophotometric analyses. Hydrodynamic performance was recorded under similar flow conditions to the lysate loading regime exploiting a negative step method with an acetone tracer (1%, v/v; [11,12]).

Table 1
Adsorbent characteristics

| | Streamline | Zirblast Agarose[a] |
|---|---|---|
| Manufacturer | Amersham Pharmacia Biotech | Birmingham Construction |
| **Properties** | | |
| *Materials of construction* | | |
| Dense material | Quartz | Zirblast[a] |
| Biocompatible matrix | 6% Agarose | 6% Agarose |
| Pore diameter[b] (nm) | <30 | <30 |
| Particle diameter[c] (μm) | 100–300 | 60–125 |
| Density ($kg/m^3$) | 1160 | 3850 |
| Ligand | DEAE | DEA |
| Small ion capacity[d] (μmol/ml settled adsorbent) | 170 | 8 |
| **Hydrodynamic performance**[e] | | |
| Height equivalent to a theoretical plate (cm) | 0.45 | 0.51 |
| Axial dispersion coefficient ($m^2/s$) | $7.5\times10^{-7}$ | $11\times10^{-7}$ |
| Bodenstein number | 67 | 53 |

[a] Zirblast Agarose (ZrA), is a pellicular adsorbent with a solid silica/zirconia composite core coated with a thin layer (<5 μm) of DEA derivatised agarose. The material was custom manufactured according to Ref. [5].
[b] Inferred from electron microscopy.
[c] Estimated by Malvern Mastersizer.
[d] Estimated by titration.
[e] Estimated by negative step acetone tracer stimulus under normal operating conditions (see Section 2.1 and Refs. [11,12]).

### 2.2. Biochemical assays

Samples were appropriately diluted into the linear range of absorbance for DNA (<0.6 absorbance) using UDB and read on a Pharmacia LKB Ultrospec III spectrophotometer at 254 nm in a 1-cm path length quartz cuvette. Electrophoretic analyses exploited a modified method of Sambrook et al. [8] using a 1% agarose in an Anachem Scotlab SL-HL electrophoresis apparatus and visualised following treatment with ethidium bromide using a TS-15E UVP ultraviolet transilluminator. Plasmid quantitation relative to serial dilutions of plasmid standards was undertaken and documented by digital camera and an IMAGO imaging system. Plasmid DNA concentration in samples was also estimated using the PicoGreen reagent according to a method developed herein from Singer et al. [9] and the manufacturer's recommendations [10].

A PicoGreen working reagent solution (PGws) was prepared by 1/500 dilution of stock solution in universal dilution buffer (UDB). Samples were diluted to correspond to the linear part of the calibration curve (0–0.4 μg/ml) freshly constructed using pure pTX0161 plasmid DNA. Equal volumes of PGws and diluted sample were mixed and incubated in the dark for 1 h at room temperature before analysis in a Perkin-Elmer LS 50B luminescence spectrometer. Duplicate samples were excited for 5 s and the emission measured at wavelengths of 485 and 520 nm, respectively, with a 5-nm slit width. Estimates of plasmid concentrations using the PicoGreen assay were also made following pre-purification of samples by Qiagen Mini-Prep procedures [13].

## 3. Results

### 3.1. Comparative plasmid recoveries

An objective of the current work was to compare the performance of an adsorbent custom designed for nano-scale particulate bioproducts [5] with those originally developed for protein adsorption and subsequently applied to the purification of viruses and plasmid DNA [4]. As discussed in Refs. [5,6,14], pore diameters of the latter (in the range 10–400 nm) are likely to strongly constrain the internal diffusive transport of nanoscale particulate bioproducts. The fluidised bed recovery of the plasmid pTX0161 (7.8 kb of dsDNA) from a complex feedstock, generated from the alkaline lysis of *E. coli* produced in microbial fermentation [4] was selected as a representative evaluation system.

Two contrasting configurations of adsorbent design were selected, whose characteristics are depicted in Fig. 1. Streamline (from Amersham Pharmacia Biotech [7]), an adsorbent containing dense quartz particles embedded in a 6% (w/v) cross-linked agarose gel, was chosen as a relatively porous adsorbent designed for protein capture but subsequently applied to the recovery of plasmid DNA [4]. The second adsorbent, Zirblast Agarose (ZrA) was custom manufactured to provide a ''pellicular'' construct comprising a solid dense core of Zirblast from SEPR (La Defense, France) laminated with a thin ''skin'' (<5 μm estimated depth) of 6% (w/v) agarose (S.C. Burton, unpublished experiments). The

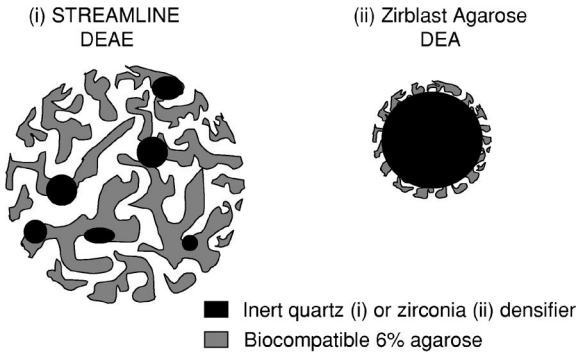


Fig. 1. Cross-sectional representation of candidate adsorbents. Detailed characteristics are given in Table 1 for adsorbents depicted in section and approximately to scale.

commercial and customised adsorbents were derivatised with anion-exchange chemistries (DEAE or DEA, respectively; see Table 1 and Ref. [5]).

Both adsorbents were evaluated under identical process conditions, in terms of contactor configuration, settled bed height (SBH), feedstock composition and volumetric flow-rate (as described in Section 2.1) to facilitate a comparison of performance with respect to fluidised bed chromatographic recovery of plasmid DNA from the crude plasmid feedstock. The chromatographic profile of each was monitored with respect to the plasmid concentration and process stream absorbance ($A_{254}$) at the contactor outlet.

### 3.2. Sample analysis

Absorbance measurements at 254 nm enabled rapid and simple estimates of plasmid concentration in pure, relatively concentrated samples. However, the sensitivity of such analyses is relatively poor (minimum detection limit of 5 μg DNA/ml [8]), whilst background absorbance from common contaminants such as proteins, other nucleic acids or phenols rapidly swamp the plasmid signal in impure samples. In contrast, agarose gel electrophoresis of samples is highly sensitive when serviced by an appropriate staining agent [15,16] and enables the visualization of different nucleic acid forms. However, accurate quantitation is difficult, requires costly gel scanning equipment [17] and is time consuming with significant sample pre-treatment. Consequently, a fluorometric method, better suited to the rapid, multiple analyses required of plasmid purification was identified and adapted for the present study. PicoGreen dsDNA reagent was preferred to established Hoechst dyes [18] because of advantages of increased sensitivity (minimum detection limit of 25 pg/ml), rapidity of assay without sample pre-treatment, specificity for double-stranded DNA without base selectivity, and minimal background fluorescence [9]. Singer et al. [9] have discussed the possible mechanism of binding of PicoGreen with reference to related dimeric cyanine dyes [19,20], which primarily intercalate when bound to oligonucleotides but also interact with DNA in other ways. Observations concerning the binding properties of PicoGreen reagent suggest that the fluores-

cence is conformation dependent, sensitive to divalent cationic salts and ionic detergents but *not* base-selective.

With respect to the analysis of the chromatographic process, the estimation of plasmid content of the crude lysate poses many problems. The lysate [4] contains plasmid together with a multitude of contaminants including genomic DNA, RNA and RNA fragments, protein, lipo-polysaccharide endotoxin and various poorly defined pigments, plus a high concentration of potassium acetate (0.8 *M*) and significant traces of sodium dodecylsulfate (SDS) at a pH of 5.5. The adsorption breakthrough and wash fractions contain varying concentrations of these solutes. Plasmid quantitation in subsequent elution samples recovered with buffers B2 and B3 is influenced by NaCl and RNA content, the latter concentrated through co-purification with plasmid DNA.

Sample pH was found to directly influence PicoGreen fluorescence, and thus the pH value of each was adjusted to 7.5 where both high emission and signal stability was achieved. In order to accommodate the wide variety of mobile phase conditions and achieve a pH of 7.5 it was both theoretically established and experimentally confirmed that a minimum 1 in 50 dilution with UDB was essential to accommodate the most extreme challenge to the assay, i.e., the 0.8 *M* potassium acetate contained in lysate feedstock at an original pH of 5.5. A 1 in 500 dilution of the reagent in UDB was adopted as the PicoGreen working solution (PGws) for the assay and the plasmid concentration in all samples was serially diluted with UDB to values less than 0.4 μg/ml plasmid. The reagent was thus in considerable excess to the plasmid concentration such that considerations of reaction equilibrium and competitive interaction of contaminants were minimised. Replicate samples were serially diluted and assayed against a calibration curve generated from pure standard plasmid with freshly prepared PGws.

Fig. 2 depicts a typical calibration of pure plasmid concentration plotted against emission intensity following treatment with PGws. The plot is characteristically linear over several orders of magnitude embracing the normal assay range (0–0.4 μg/ml plasmid). Previous workers [9,21] have shown that NaCl concentration may influence the PicoGreen

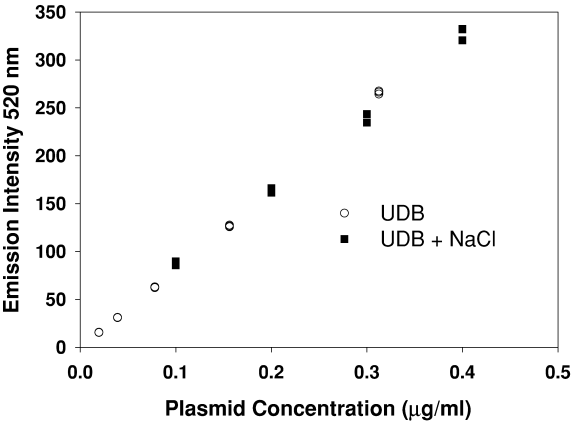


Fig. 2. PicoGreen calibration for plasmid DNA in the presence/absence of NaCl. Known masses of plasmid pTx 0161 in UDB (○) and UDB containing 2.0 *M* NaCl (■) at pH 7.5 were further diluted with UDB and mixed with equal volumes of PGws (1 in 500 dilution in UDB of the original stock solution). The samples were excited at 485 nm in a fluorimeter and emission intensity read at 520 nm (see Section 2.2). Error between replicate samples was routinely less than 2% with $R^2 > 0.999$ for correlation analyses.

assay, the former quoting a 30% quenching of emission signals for samples containing 200 m*M* NaCl. However, the standard 1 in 50 dilution of sample adopted in this study ensured that there was no discernible difference between the pure plasmid standard and samples containing 2.0 *M* NaCl (refer to Fig. 2). Similarly, the influence of up to 0.8 *M* potassium acetate was minimised by this same dilution (data not shown).

The complex nature of the lysate feedstock meant that interactions between the process stream contaminants and the assay system could only be realistically tested in purification experiments. As an example, Fig. 3 shows the relationship of $C/C_o$ (where $C$ is the concentration in the effluent fraction and $C_o$ is the concentration in the lysate feedstock) with volume of applied feedstock exploiting ZrA-DEA in fluidised bed mode. The close correspondence between estimates of plasmid DNA concentrations by PicoGreen assay and those from gel electrophoresis were encouraging and confirms that the former offers a direct, rapid and reproducible measure of the plasmid content of breakthrough fractions. Furthermore, the various concentrations of SDS, proteins, lipo-polysaccharide and endotoxin

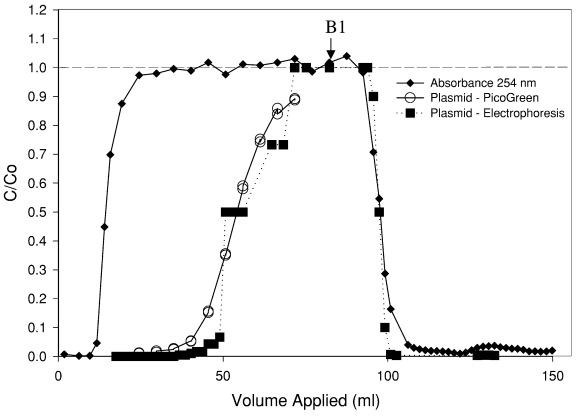


Fig. 3. Chromatographic breakthrough analysis for the ZrA DEA adsorbent. The chromatographic breakthrough is plotted in respect of absorbance at 254 nm (♦), plasmid concentration (estimated by PicoGreen assay (○)) and gel electrophoretic comparison with a serially diluted standard (■) as $C/C_o$ against applied volume where $C$ is the concentration in the effluent fraction and $C_o$ is the concentration in the initial lysate. ZrA DEA was challenged with lysate (85 ml) in a fluidised bed contactor expanded to 10% at a flow-rate of 0.9 ml/min (Section 2.1).

were too low to antagonise the PicoGreen assay. Notably, on-line spectrophotometric analyses gave no specific indication of the initiation or extent of plasmid breakthrough, but rather a non-selective trace of 254 nm absorbing contaminants in the bed effluent. In fact, the plasmid concentration in the feedstock at loading (~23 μg/ml plasmid) would be theoretically expected [22] to contribute less than 2% of the initial $A_{254}$ values which were dominated by the contribution of contaminants. However, it would appear that the PicoGreen assay over-estimated the plasmid content of sample fractions close to breakthrough for Zr DEA, whereas this was not seen with Streamline DEAE. Inspection of the ZrA DEA fractions by gel electrophoresis (data not shown for this run, but refer to Fig. 9) revealed a high concentration of RNA assumed to be retarded and concentrated due to anion-exchange interactions with the adsorbent. Whilst this observation had little effect on the overall process mass balance, or estimates of the dynamic breakthrough capacity at $C/C_o = 0.1$, the consequences for determination of the plasmid content of salt eluted fractions in the presence of co-purifying nucleic acid contaminants (e.g., RNA fragments) are more significant.

As shown in Fig. 4a, PicoGreen positively interacts with RNA Type VI (from Torula yeast), to produce an emission response which is diminished by incubation with RNAase A (from Qiagen Mini-Prep Kit) (see Fig. 4b). These figures confirm that RNA can influence PicoGreen estimates of dsDNA, but that on a concentration basis the emission is only 2% of that for plasmid. As the RNA is fragmented, the PicoGreen emission declines further but the $A_{254}$ signal remains constant. The degree of fragmentation

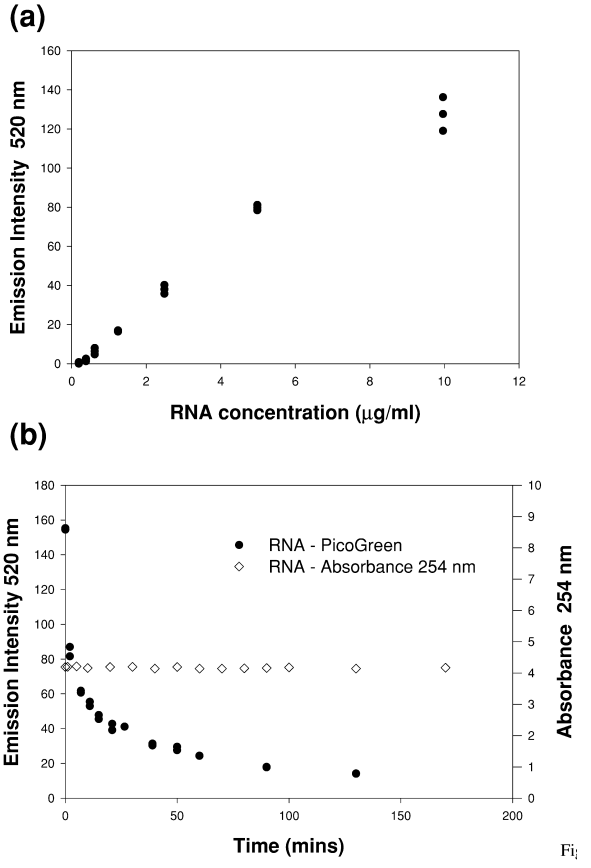


Fig. 4. PicoGreen calibration for RNA concentrations. (a) Known masses of Torula yeast RNA Type VI were diluted with UDB and mixed with equal volumes of PGws (1 in 500 dilution in UDB of the original stock solution). The samples were excited at 485 nm in a fluorimeter and emission intensity read at 520 nm (Section 2.2). (b) A 0.933-mg/ml concentration of Torula yeast RNA Type VI was digested with 1.01 μg/ml RNAase at 24°C. Samples were assayed for RNA as in (a) (●). The absorbance (254 nm) for each sample was also recorded (◇). RNAase did not influence a PicoGreen control or display significant spectroscopic adsorption.

and concentration of *E. coli* RNA in the feedstock and subsequent 0.5 and 2.0 *M* NaCl elution peaks was not known for representative purifications such as those depicted in Figs. 3, 5 and 6. Assuming that

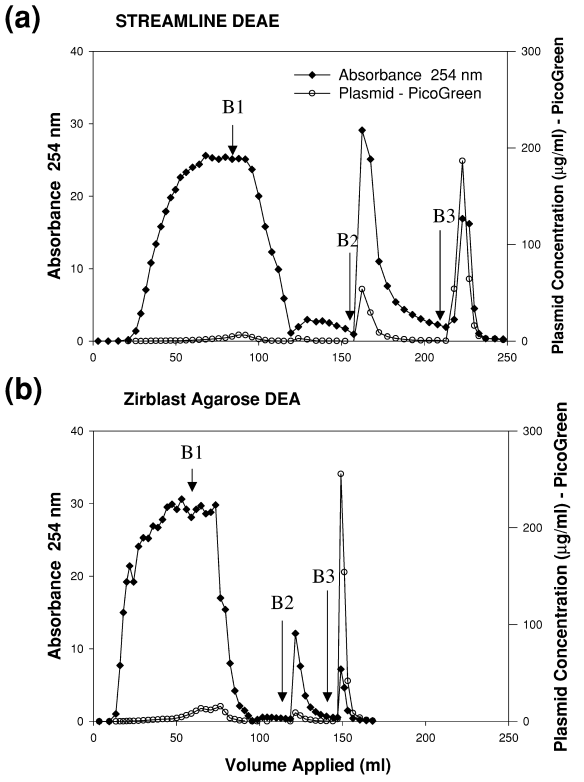


Fig. 6. Full chromatographic analyses of the comparative performance of Streamline DEAE and ZrA DEA adsorbents. (a) The chromatographic profile for Streamline DEAE is plotted in respect of absorbance at 254 nm (♦) and plasmid concentration (○) (estimated by PicoGreen assay) against volumetric throughput. A 75-ml challenge of lysate was contacted with a pre-equilibrated Streamline DEAE adsorbent bed expanded to 58% by a flow-rate of 1.0 ml/min in a 1.0-cm diameter Omnifit contactor. Equilibration buffer (B1) was then applied under similar flow conditions to wash contaminants from the bed before the bed was collapsed by flow reversal into a packed configuration for elution. A wash step with 0.5 *M* NaCl (B2) removed loosely bound RNA, followed by product elution with 2.0 *M* NaCl (B3). The bed was then cleaned with acid and base before re-equilibration and re-expansion with equilibration buffer (B1) in preparation for further cycles. (b) Chromatographic profile for ZrA DEA as in (a) plotting absorbance at 254 nm (♦) and plasmid concentration. A 65-ml challenge of lysate was contacted with a pre-equilibrated ZrA DEA adsorbent bed expanded to 12% by a flow-rate of 1.0 ml/min in a 1.0-cm diameter Omnifit contactor, operated as described in (a).

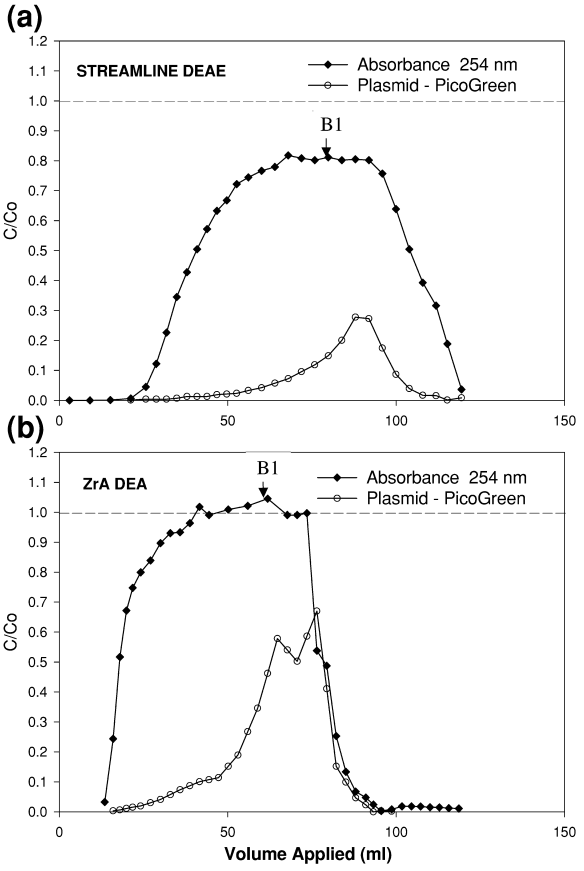


Fig. 5. Comparative chromatographic breakthrough profile for Streamline DEAE and ZrA DEA adsorbents. (a) The chromatographic breakthrough is plotted in respect of absorbance at 254 nm (♦) and plasmid concentration (○) (estimated by PicoGreen assay) as $C/C_o$ against applied volume where $C$ is the concentration in the effluent fraction and $C_o$ is the concentration in the initial lysate. A 75-ml challenge of lysate was contacted with a pre-equilibrated Streamline DEAE adsorbent bed expanded to 58% by a flow-rate of 1.0 ml/min in a 1.0-cm diameter Omnifit contactor. Equilibration buffer (B1) was then applied to wash contaminants from the bed (Section 2.1). (b) The chromatographic breakthrough analysis plotted as in (a) for absorbance at 254 nm (♦) and plasmid concentration (○). A 65-ml challenge of lysate was contacted with a pre-equilibrated ZrA DEA adsorbent bed expanded to 12% by a flow-rate of 1.0 ml/min in a 1.0-cm diameter Omnifit contactor, as indicated in (a).

(i) the NaCl elution peaks were comprised almost exclusively of nucleic acids, (ii) the influence of RNA on PicoGreen emission intensity is small, (iii) the relation between $A_{254}$ and concentration of plasmid DNA or RNA are both constant [20] and

(iv) $A_{254}$ is independent of the RNA fragment size (see Fig. 4b), a simple mass balance based on PicoGreen and absorbance (254 nm) estimation of plasmid and RNA concentrations was derived for the system. This yields both a measure of the plasmid concentration and sample purity (expressed for convenience as the ratio of PicoGreen plasmid and $A_{254}$ estimates) in terms of total nucleic acid content, assuming that the type and size range of RNA fragments remains constant in all samples. Such an assumption is reasonable considering that the feedstock came from a common source for all the experiments and that the ligand chemistry was similar for both adsorbents. Recovery and measurement of the plasmid concentration in the contactor effluent generated from cleaning operations with NaOH and HCl proved impossible to accurately achieve with the assays applied in this work.

### *3.3. Hydrodynamics of fluidised bed operations*

The two adsorbent materials, Streamline DEAE and ZrA DEA, operated in the same fluidised bed contactor at equivalent volumetric liquid throughput exhibited similar hydrodynamic behaviour in terms of estimates of axial dispersion, height equivalent of a theoretical plate (HETP) and Bodenstein number (Bo) when measured with acetone as the tracer molecule (refer to Table1 where Bo represents the sum of the superficial fluid velocity and expanded bed height divided by the coefficient of axial dispersion). The Bodenstein number is commonly used to express the combined states of liquid dispersion and fluidisation behaviour, where numbers in excess of 50 represent satisfactory contactor and adsorbent performance [23–25]. However, the recent work of Lan et al. [23] indicates that such commonly recorded quantities [24,25] do not impact heavily on the practical chromatographic performance, although a stable, classified, bed is generally to be preferred [26].

Particle diameter ratios for glass beads (smallest: largest $>2.2$ have been found to sufficiently suppress adverse mixing effects. Streamline DEAE and ZrA DEA, with respective particle ratios of approximately 3 and 1.9, appeared to rapidly establish stable fluidised beds. Both adsorbents expand linearly with increasing flow velocity, but, the expansion of ZrA

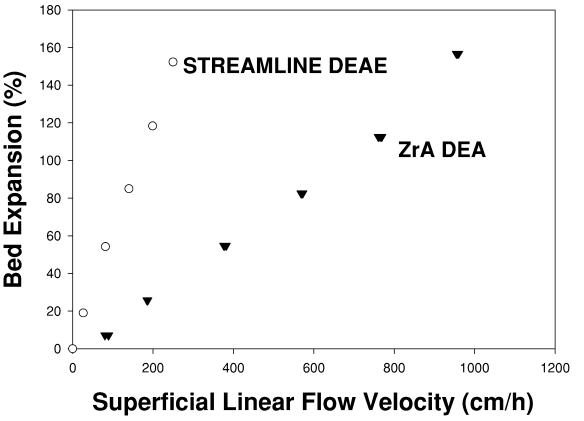


Fig. 7. Fluidised bed expansion behaviour for Streamline and ZrA adsorbents. Equilibration buffer (B1) was contacted with 15 cm settled bed height (SBH) of adsorbent (Streamline DEAE (○) and ZrA DEA (▼) in a 1.0-cm diameter Omnifit contactor at various flow velocities at room temperature. Starting at a maximum flow velocity, the bed was allowed to stabilise for 1 h before the new bed height was recorded. Flow velocity was then incrementally reduced and the process repeated.

DEA was nearly four times less than that of Streamline DEAE at a given fluidisation velocity (see Fig. 7). The settling velocity of the adsorbent is related to (i) the density difference between the particle and the fluid phase and (ii) the square of the particle diameter [27]. ZrA-DEA, despite having a characteristic diameter (60–125 μm) approximately half that of Streamline DEAE (100–300 μm), exhibited greater negative buoyancy by virtue of the dense Zirblast core which contributes a large proportion ($>80\%$) of the particle volume (refer to Table 1). The opportunity to significantly increase the density of a porous particle, largely inundated by process liquor, is limited, especially when the base matrix is constructed from agarose, dextran, cellulose and synthetic polymers with densities close to that of water. Only limited work has been published on the influence of bed expansion on processing characteristics [28,29]. However, the ability of an adsorbent to form a stable fluidised bed at high feedstock throughput velocities has important processing implications [5].

Assuming sphericity for each particle, ZrA DEA has approximately one-eighth of the porous volume and a quarter of the external surface area of Streamline DEAE because the ratio of external surface area

to volume increases with diminishing particle diameter. However, the amount of external surface area available per unit volume of settled ZrA DEA adsorbent (assuming constant voidage) is greater than that of Streamline DEAE since more of the former can be packed into a unit volume. Thus, the capture of plasmid DNA that binds exclusively to the external surfaces of small, dense and solid particles such as ZrA DEA [5] would appear to have an advantage in terms of capacity. Further, there are practical benefits in terms of ligand utilisation since *only* the surface physically available for product binding requires derivatisation. Thus, although the small ion capacity for a common settled volume of ZrA DEA appears to be less than 5% of that measured under identical conditions for Streamline DEAE (refer to Table 1), the exclusive location of the DEA ligand at the surface of the ZrA particle surface governs that the local ligand concentrations (accessible to the plasmid DNA) are likely to be approximately equivalent.

The batch processes commonly exploited for the chemical modification of adsorbents mean that the internal surfaces of porous adsorbents (such as Streamline) will carry large quantities of ligand which will not be exploited in adsorption/desorption operations with nanoparticulate products (refer to Fig. 1). This may have significant economic consequences for the coming generation of highly selective ligands (sophisticated chemical, peptide or oligonucleotide assemblies specific for nanoparticles [3,5,13,30]). Moreover, where repetitive use of adsorbents is required, the mandatory development of validated cleaning protocols for surfaces which contribute no positive product adsorption/desorption to the process (but which accumulate impurities; see later) represents an inefficient exploitation of resources.

### *3.4. Plasmid purification: breakthrough profiles*

Consideration of the breakthrough analyses for Streamline DEAE and ZrA DEA operated under identical process conditions indicates, by virtue of non-equality of input and output concentrations ($C/C_o = 1$), the retention of process contaminants (e.g., linear fragments of DNA and RNA, protein, pigments etc) within the porous interior of Streamline DEAE (contrast $A_{254}$ and PicoGreen profiles in Fig. 5a,b). Furthermore, the presence of RNA fragments cannot be identified in electrophoretic analyses of breakthrough fractions from Streamline DEAE (a typical example being lanes 2 and 3 in Fig. 9), whereas they can in similar samples from ZrA-DEA (lanes 4–8). In terms of absorbance analyses at 254 nm, the signal breakthrough initiates earlier and distinctly more sharply for ZrA DEA as compared with Streamline DEAE and $C/C_o$ (effluent/feedstock values) reaches unity. Porous Streamline has a much greater internal surface area available for the adsorption of low-molecular mass contaminants (but *not* plasmid) as compared to the pellicular ZrA adsorbent (refer to Fig. 1 and Table1). Consequently, on washing to baseline absorbance, ZrA DEA was rapidly purged of non- and weakly binding contaminants and plasmid as evidenced by the coincidence of the $A_{254}$ and PicoGreen traces in Fig. 5b. The volume of buffer B1 required to purge the extra particle and interstitial volumes of Streamline DEAE of contaminants (as judged by effluent absorbance at 254 nm in Fig. 5a) far exceeded that required to eliminate unbound plasmid from the outer particle surface of both adsorbent particles (compare $A_{254}$ and PicoGreen traces in Fig. 5a,b).

PicoGreen analyses indicate that Streamline DEAE had a greater dynamic binding capacity (approximately 106 μg plasmid/ml settled adsorbent at $C/C_o = 0.1$) than ZrA DEA (approximately 57 μg plasmid/ml settled adsorbent at $C/C_o = 0.1$). This may reflect differences in the ligand concentration and surface topography accessible to the product for the two adsorbents. Confocal microscopic imaging of plasmid DNA bound to Streamline DEAE and subsequently stained with PicoGreen revealed plasmid to be bound only around the perimeter of the particles (refer to Fig. 8). Sectional scanning indicated that plasmid penetrated into the 6% agarose component of Streamline to an apparent depth less than 5 μm, in line with similar analyses by Ljunglof et al. [31]. This might be interpreted in terms of surface ''roughness'' rather than true penetration, since negligible electrophoretic migration into agarose gels (2%, w/w) was consistently observed for the 7.8 kb plasmid pTX 01061 (data not shown). Breakthrough curves for contaminants ($A_{254}$) and for plasmid (PicoGreen) were less steep for Streamline

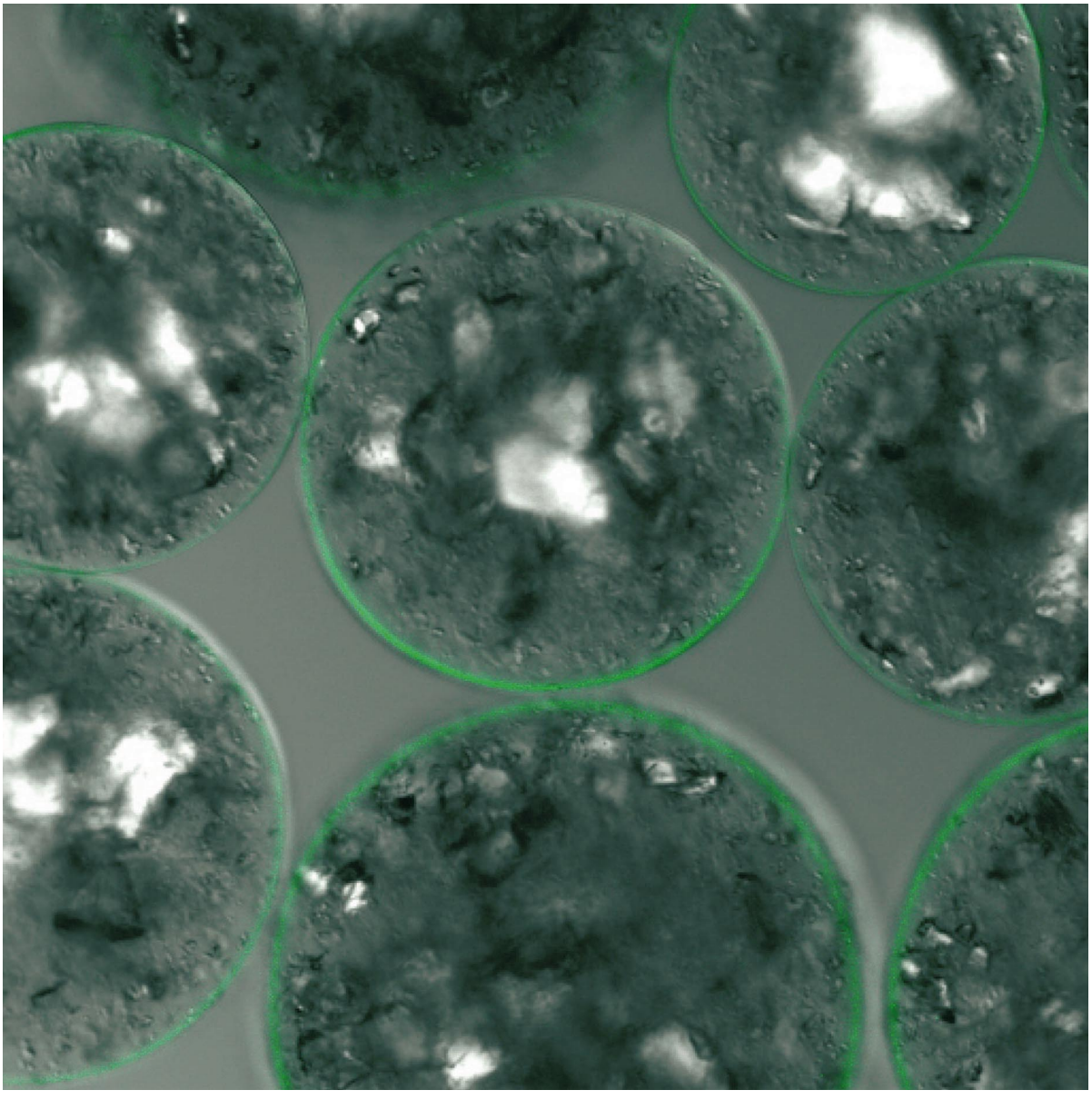

Fig. 8. Combined transmission and fluorescence confocal image of plasmid bound to Streamline DEAE. Streamline DEAE adsorbent (0.2 ml) was exposed to 5 ml pure plasmid pTX0161 (20 μg/ml plasmid in UDB) for 12 h in a plastic universal bottle at room temperature with gentle mixing. Recovered adsorbent was washed three times with an excess of UDB to remove unbound plasmid and then stained with PGws before visualisation using a Zeiss LSM 510 laser scanning confocal microscope. Transmission and fluorescent wavelengths were 543 and 488 nm, respectively.

DEAE than ZrA DEA, indicating that the pellicle of the latter was more rapidly saturated than those adsorbent surfaces available in Streamline (compare Fig. 5a,b). The shallow depth of the ZrA pellicle was further confirmed by the failure of adequate visualisation in confocal microscopic analysis.

### 3.5. Plasmid purification: elution profiles

Full process cycles for plasmid purification exploiting Streamline DEAE and ZrA DEA are depicted in Fig. 6a,b). The initial breakthrough profiles (loading and wash) in fluidised bed mode summarise performances depicted in Fig. 5a,b and analysed in detail above. The salt wash (buffer B2), deployed in packed bed mode with 0.5 *M* NaCl (buffer B2) to eliminate weakly bound contaminants, yielded a large peak of absorbance (254 nm) for Streamline DEAE with considerable tailing of the signal representative of a purge of molecular contaminants from the interstitial pore volume. Increase of the salt concentration of B2 to 0.5 *M* NaCl failed to significantly reduce this tailing, and initiated unwanted desorption and loss of plasmid DNA product (data not shown). In order to avoid the excessive buffer volumes required to achieve baseline absorbance values (estimated to exceed 10 settled bed volumes (SBVs) from interpolation of Fig. 6a) and reduce process time, product elution with 2.0 *M* NaCl was initiated (buffer B3) at an effluent absorbance of 2.0 ($A_{254}$) such that some residual contaminants co-eluted with the plasmid DNA. In similar operations, ZrA DEA exhibited a small absorbance peak with minor tailing and baseline absorbance ($A_{254}$) was achieved with less than 1.5 SBV of buffer B2. The pellicular skin of anion-exchange agarose laminated upon the solid Zirblast core accumulated fewer contaminants during loading, and was rapidly purged with buffers B1 and B2 to the benefit of subsequent product purity following elution with B3. PicoGreen analysis of the plasmid content of the buffer B2 wash fractions indicated significant product loss from Streamline DEAE (26% of that bound based on PicoGreen analyses) as compared to 4% for ZrA DEA. Gel electrophoretic analysis of these fractions (Fig. 9, lanes 10 and 9, respectively) confirmed that those arising from Streamline DEAE contained significant quantities of both plasmid and RNA, whilst those from ZrA DEA contained only RNA.

Both adsorbents exhibited a discrete peak of eluted product in 2.0 *M* NaCl (buffer B3) following PicoGreen analyses, although that from the ZrA DEA peak of PicoGreen was more pronounced, concentrated and exhibited a higher purity of plasmid DNA (see Table 2 and Fig. 9, lanes 11 and 12). At

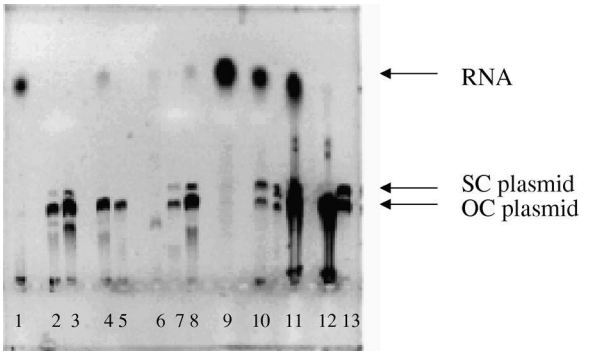


Fig. 9. Gel electrophoresis of effluent fractions. Electrophoresis gel prepared according to the method of Sambrook et al. [8] stained with ethidium bromide. Sample concentrations were overloaded to facilitate RNA visualisation. Positions of supercoiled (SC) and open-circular (OC) plasmid forms and RNA are indicated by arrows. Lanes: (1) RNA type VI standard; (2,3) Streamline DEAE breakthrough fractions sampled at ~60 and 70 ml, respectively (see Fig. 5a); (4,5) ZrA DEA breakthrough fractions sampled at ~ 56 and 68 ml, respectively (see Fig. 3); (6–8) ZrA DEA breakthrough fractions sampled at ~33, 50 and 62 ml, respectively (see Fig. 5b); (9) NaCl 0.5 *M* elution (B2) from ZrA DEA sampled at ~122 ml and concentrated ×4 (see Fig. 6b); (10) NaCl 0.5 *M* elution (B2) from Streamline DEAE sampled at ~167 ml (see Fig. 6a); (11) NaCl 2.0 *M* elution (B3) from Streamline DEAE sampled at ~218 ml (see Fig. 6a); (12) NaCl 2.0 *M* elution (B3) from ZrA DEA sampled at ~149 ml (see Fig. 6b); (13) pure plasmid pTx 0161 standard.

experimental scale (SBV=12 ml adsorbent), the time for a process cycle for ZrA DEA (including cleaning and regeneration treatments) was significantly reduced by more than 60% when compared to Streamline DEAE (discussed in Ref. [5]). Up-scaled process cycles would be expected to reap similar benefits of reduced timescale and buffer consumption.

### 3.6. Plasmid purification: mass balances and purity

The process characteristics for the fluidised bed operation of the two absorbents in plasmid recovery are outlined in Table 2. Closure of the mass balances for plasmid DNA (based on a lysate challenge containing ~23 μg/ml of plasmid confirmed by Qiagen purification and quantification with PicoGreen) approximated to 100% for both adsorbents. Streamline DEAE exhibited nearly double the dynamic binding capacity for plasmid (see Table 2)

Table 2
Plasmid mass balance for the various stages of fluidised bed purification

| | Volume[a] (ml) | Plasmid[d] concentration (μg/ml) | Plasmid mass[d] balance (%) | Plasmid[c] recovery (%) | Purity[b] ratio (%) |
|---|---|---|---|---|---|
| *Streamline DEAE* | | | | | |
| Load | 75 | 23 | – | – | – |
| Breakthrough and wash | 108 | ND | 11 | – | – |
| 0.5 *M* NaCl wash | >100[e] | 11 | 24 | 26 | 0.7 |
| 2.0 *M* NaCl elution | 30 | 38 | 67 | 76 | 9 |
| Total | 240 | – | 102 | 102 | – |
| *ZrA DEA* | | | | | |
| Load | 65 | 23 | – | – | |
| Breakthrough and wash | 84 | ND | 25 | – | – |
| 0.5 *M* NaCl wash | 15 | 3 | 4 | 6 | – |
| 2.0 *M* NaCl elution | 12 | 79 | 67 | 90 | 0.7 |
| Total | 150 | – | 96 | 96 | – |

Lysate containing approximately 23 μg/ml plasmid DNA was applied to 15 cm SBH of adsorbent in a 1-cm diameter Omnifit contactor at a feed rate of 1 ml/min. Adsorbent bed expansions in loading were 12 and 58% for ZrA DEAE and Streamline DEAE, respectively. All estimations are based on collection of entire absorbance 254-nm peaks as depicted in Fig. 6a,b.

[a] Adjusted for system ''dead volume''.

[b] Expressed as plasmid concentration (PicoGreen) divided by $A_{254}$ for the pooled elution peaks.

[c] Expressed as percent of plasmid recovered in the 2.0 *M* NaCl elution peak relative to that bound to the adsorbent during loading.

[d] PicoGreen assay.

[e] Extrapolated from Fig. 6a.

which may reflect differences in local available ligand concentration in the two disparate particle geometries. However, product recoveries with 2.0 *M* NaCl expressed relative to estimates of bound plasmid were higher for ZrA DEA. This might reflect a constraint of diffusive release even where limited penetration of the external particle surface of Streamlinie DEAE may have been achieved. The overall performance of Streamline DEAE was characterised by losses in buffer B2 (24% of bound material), inferior product purity (see Table 2 and Fig. 9, lanes 11 and 12) and extended process volumes/times (refer to Fig. 6).

## 4. Concluding discussion

Adopting conventional porous adsorbent designs (with specifications appropriate for protein recovery) for the purification of nanoscale bioparticulate products (20–200+ nm diameter) creates a number of major processing difficulties. Such problems, common to both fluidised and fixed bed applications, arise from the retention of significant quantities of impurities from crude feedstocks in the porous interior of adsorbents which, by virtue of size-exclusion, is not accessible to the product. Complete purging of this volume requires extended processing times, whilst pragmatic compromise on the extent of the purge reduces product purity (see Fig. 6a). Replacement of the porous interior with an impenetrable core (as in ZrA DEA) significantly enhances the selectivity of product recovery by reducing the quantity of contaminating impurities in the mass balance post-adsorption. Furthermore, the adoption of a dense core enables an improved control of particle fluidisation throughout the process cycle. Controlled particle geometry and increased density will facilitate the intensification of fluidised bed operations in terms of (i) increased product throughput, (ii) reduced sensitivity to process fluid viscosity and/or (iii) minimal bed expansion (i.e., contactor volume). Bierau et al. and Hamilton et al. [32,33] have proposed novel feedstock contacting applica-

tions that would capitalize on the rapid loading, elution and regeneration characteristics of such pellicular adsorbents operated with crude feedstocks.

However, in terms of operating capacity for plasmid DNA, it is difficult to reconcile the performance of the adsorbent materials with the multigram quantities forecast for the gene therapy applications (discussed in Refs. [1–3]). Surface chemistries might be developed in order to achieve improved adsorption/desorption performances. Although process conditions were not exhaustively optimized in the present study, differences in the performance of the two adsorbents when operated with common protocols indicate that the local ligand concentration (i.e., that seen by the product) and elution conditions are likely to be important factors, respectively, in adsorption and desorption. There is a fine balance in maximizing binding capacity and product recovery where increasing the former (through attention to ligand concentration) may promote irreversible binding of product and impurities to the adsorbent. In contrast, favouring the latter, by establishing weaker interactions, risks product loss in the flow through at adsorption or in pre-elution washes. However, there remains the limitation of the amount of surface area available for product binding. Smaller adsorbent diameters would enhance product adsorption per unit volume of settled adsorbent, but the core would need an increased density to operate well in a fluidised bed contactor. Other particle configurations, such as ''super porous'' or ''tentacular'' geometries [34–37] might address this issue, as could the enhancement of surface topology or ''roughness''. However, it is likely that a combination of the factors described here, optimized for generic product and process needs, will be required. For example, a high capacity adsorbent that achieves limited product/impurity fractionation might meet the needs of a primary capture step, whereas in other circumstances the achievement of a highly pure product can counterbalance reduced recoveries.

We conclude from the present study that two contrasting geometries of adsorbent solid-phase superficially exhibit similar behaviour in the recovery of plasmid DNA from *E. coli* extracts prepared by chemical lysis and coarse filtration. The behaviour of both adsorbents is characterised by size exclusion of nanoscale products, which restricts adsorption to the outer surface of particulate solid-phases. However, rigorous development of PicoGreen analyses to enable robust estimates of plasmid DNA in the presence of system antagonists (salts, pH variation, RNA, linear DNA, etc.) has, in tandem with electrophoretic analyses, demonstrated significant differences in performance for the two adsorbents. In particular, the near solid ZrA DEA adsorbent (possessed of a thin agarose pellicle) adsorbs fewer anionic contaminants (RNA, DNA, etc.) as confirmed by their strong presence in PicoGreen analyses of breakthrough fractions at loading. In contrast, Streamline DEAE has little of that presence and must be assumed to be accumulating such materials in the interstitial pore volume during the adsorption stage of the process. This is confirmed in part by wash treatments with 0.5 *M* NaCl (buffer B2) where the PicoGreen signal is more heavily influenced by the presence of RNA in the effluent from Streamline DEAE (compare lanes 9 and 10 in Fig. 9). In addition, the internal volume of this adsorbent requires considerably more washing and pre-elution feedstock to displace such contaminants (compare Fig. 6a,b). The near solid geometry of ZrA DEA enhances the elution yield, concentration and purity of recovered plasmid DNA in a manner not seen with the porous adsorbents in this and other studies [5]. When such micro-pellicular materials are (i) further diminished in particle diameter, (ii) enhanced in particle density, and (iii) derivatised with more selective chemical ligands, these advantages could be augmented by properties of increased product capacity and throughput together with economies of assembly and operation. Such conclusions have a generic relevance to the selective recovery and manufacture of all nanoparticulate products (viruses, plasmids, virus-like particles, vaccine components, etc.) sourced in biological systems.

## 5. Nomenclature

| | |
|---|---|
| $A_{254}$ | absorbance at 254 nm |
| B1 | equilibration buffer |
| B2 | pre-elution buffer |
| B3 | elution buffer |
| Bo | Bodenstein number |
| EDTA | ethylene diamine tetra-acetic acid |

| | |
|---|---|
| DEA | diethylamine |
| DEAE | diethylaminoethyl |
| dsDNA | double-stranded deoxyribonucleic acid |
| HETP | height equivalent of a theoretical plate |
| OCP | open circular plasmid |
| PGws | PicoGreen working solution |
| SBH | settled bed height |
| SBV | settled bed volume |
| SCP | super coiled plasmid |
| UDB | universal dilution buffer |

## Acknowledgements

This work was funded by a BBSRC/DTI LINK programme in Biochemical Engineering in collaboration with Whatman International Ltd. and Cobra Therapeutics Ltd.

## References

[1] D.M. Prazeres, G.N.M. Ferreira, G.A. Monteiro, C.L. Cooney, J.M.S. Cabral, Trends Biotechnol. 17 (1999) 169.
[2] S.M. Levy, R.D. O'Kennedy, P. Ayazi-Shamlou, P. Dunnhill, Trends Biotechnol. 18 (2000) 296.
[3] A. Lyddiatt, D. A O'Sullivan, Curr. Opin. Biotechnol. 9 (1998) 177.
[4] D.L. Varley, A.G. Hitchcock, A.M. Weiss, W.A. Horler, R. Cowell, L. Peddie, G.S. Sharpe, D.R. Thatcher, J.A. Hanak, Bioseparation 8 (1999) 209.
[5] Z. Zhang, S.C. Burton, S. Williams, E. Thwaites, A. Lyddiatt, Bioseparation 10 (2001) 113.
[6] D.M.F. Prazeres, T. Schluep, C. Cooney, J. Chromatogr. A 806 (1998) 31.
[7] H.A. Chase, Trends Biotechnol. 12 (1994) 296.
[8] J. Sambrook, E.F. Fritsch, T. Maniatis, in: Molecular Cloning: A Laboratory Manual, Cold Spring Harbour Laboratory Press, Cold Spring, NY, 1989.
[9] V.L. Singer, L.J. Jones, S.T. Yue, R.P. Haugland, Anal. Biochem. 249 (1997) 228.
[10] Molecular Probes Technical Notes, Eugene, OR, US, 2000.
[11] A.K.B. Frej, H.J. Johansson, P. Leijon, Bioproc. Eng. 16 (1997) 57.
[12] J. Thoemmes, M. Weiher, A. Karau, M.-R. Kula, Biotechnol. Bioeng. 48 (1995) 367.
[13] Qiagen Ltd, in: Qiagen Plasmid Purification Handbook, Qiagen, Crawley, UK, 1999.
[14] G.M.B. Braas, P.F. Searle, N.K.H. Slater, A. Lyddiatt, Bioseparation 6 (1996) 211.
[15] P. Sharp, B. Sugden, J. Sambrook, J. Biochem. 12 (1973) 3055.
[16] J.R. Stothard, I.A. Frame, M.A. Miles, Anal. Biochem. 253 (1997) 262.
[17] S.J. Ahn, J. Costa, J.R. Emanuel, Nucleic Acids Res. 24 (1996) 2623.
[18] C. Cesarone, C. Bolognesi, L. Santi, Anal. Biochem. 100 (1979) 188.
[19] E.J. Larson, J.R. Hakovirta, H. Cai, J.H. Jett, S. Burde, R.A. Keller, B.L. Marrone, Cytometry 41 (2000) 208.
[20] P.H. Spielmann, D.E. Wemmer, J.P. Jacobsen, Biochemistry 34 (1995) 8542.
[21] P. Murikami, M.T. McCaman, Anal. Biochem. 274 (1999) 283.
[22] K. Wilson, J. Walker, in: Principles and Techniques of Practical Biochemistry, Cambridge University Press, Cambridge, 2000.
[23] J.C.-W. Lan, G.E. Hamilton, A. Lyddiatt, Bioseparation 8 (1999) 43.
[24] F.B. Anspach, D. Curbelo, R. Hartmann, G. Garke, W.-D. Deckwer, J. Chromatogr. A 865 (1999) 129.
[25] A. Karau, J. Benken, J. Thömmes, M.-R. Kula, Biotechnol. Bioeng. 55 (1997) 54.
[26] M.R. Al-Dibouni, J. Garside, Trans. Inst. Chem. Eng. 57 (1979) 94.
[27] G.G. Stokes, Trans. Camb. Phil. Soc. 9 (1851) 8.
[28] H.A. Chase, Trends Biotechnol. 12 (1994) 296.
[29] J.D. Breccia, R. Hatti-Kaul, G.R. Castro, F. Sineriz, Bioseparation 8 (1999) 273.
[30] T. Schluep, C.L. Cooney, Bioseparation 7 (1999) 317.
[31] A. Ljunglof, P. Bergvall, R. Bhikhabhai, R. Hjorth, J. Chromatogr. A 844 (1999) 129.
[32] H. Bierau, Z. Zhang, A. Lyddiatt, J. Chem. Technol. Biotechnol. 74 (1999) 208.
[33] G.E. Hamilton, P.H. Morton, T.W. Young, A. Lyddiatt, Biotech. Bioeng. 64 (1999) 310.
[34] P.-E. Gustavsson, P.-O. Larsson, J. Chromatogr. A 734 (1996) 231.
[35] Data File 18-1123-81, High Capacity Expanded Bed Adsorption, Pharmacia Biotech, Uppsala, 1997.
[36] Catalogue W 214154, Fractogel EMD Process Media, Merck KGaA, Darmstadt, 1999.
[37] A. Pai, S. Gondkar, S. Sundaram, A. Lali, Bioseparation 8 (1999) 131.